Potential distribution of *Asplenium prolongatum* in China and its response to future climate change

Plant Biosystems

Online Resource 1 · Supplementary methods, tables and figures

Xinyi Liu, Jinchuan Guo, Wanbo Xing, Yan Zhang, Xiao-su Xiang and Qingshan Yang

Corresponding author: Qingshan Yang; College of Pharmacy, Anhui University of Chinese Medicine, Hefei 230012, China; yqssyx2008@163.com

Methods S1-S3; Tables S1-S4; Figs S1-S8

Companion files: Online Resource 2 contains Supplementary Data 1 (occurrence and model-results workbook). Online Resource 3 contains Supplementary Data 2 (analysis code and supporting calculations).

Potential distribution of *Asplenium prolongatum* in China and its response to future climate change

Supplementary material

This document contains Supplementary Methods S1-S3, Tables S1-S4 and Figures S1–S8. Individual occurrence records, Anhui specimen information, the predictor inventory and model results are provided in Supplementary Data 1. Analysis scripts, slope calculations and algorithm verification are provided in Supplementary Data 2. The data files accompany this article as Online Resources 2 and 3. Software and source-file details are provided in Methods S3.

Supplementary Methods S1. Model configurations and thresholds

S1.1 Parameter selection and spatial evaluation

Parameter selection for the full dataset used 185 calibration records and 61 evaluation records. The 279 candidate configurations were first screened by partial ROC (pROC) significance and evaluation omission rate, then ranked by AICc, yielding a regularization multiplier (RM) of 2 and quadratic and product (QP) features. Evaluation under this random split was used for model selection.

For outer spatial evaluation, the 246 records were divided at the median longitude and latitude into southwestern, southeastern, northwestern and northeastern folds. With each fold withheld in turn, the outer training sets contained 199, 170, 170 and 199 records. Their inner random training/evaluation splits contained 149/50, 128/42, 128/42 and 149/50 records, respectively, with random seeds 20260831–20260834. The inner splits were not spatially blocked. Each selected configuration was then refitted using its corresponding outer training set, and test records were always drawn from the withheld spatial fold. The predictor set was held constant, while parameter selection was performed within each outer training set.

The fixed-QP spatial diagnostic and nested tuning used the same outer folds. The former retained RM = 2 with QP features, whereas the latter selected RM/feature-class (FC) combinations of 1.5/LT, 0.5/P, 0.1/LQ and 2/QPT across the four folds. These procedures evaluated different model specifications, and their AUC and omission rates were summarized separately. The maximum training sensitivity plus specificity (MTSPS) thresholds of the nested outer models were 0.2382, 0.2760, 0.1087 and 0.2183, respectively. Each threshold was obtained from its corresponding training model; the national tenfold ensemble threshold was not applied to these folds.

The grouped Boyce index used 10 quantile bins of background predictions to partition suitability scores. Within each bin, the proportion of test occurrences was divided by the proportion of background pixels to obtain the ratio of observed to expected occurrence frequencies (P/E). The fold-specific index was the Spearman correlation between bin midpoints and P/E. This fixed-bin algorithm differs from the moving-window continuous Boyce index. Overall AUC was weighted by the number of test records, pooled omission was calculated as the total number of omitted records divided by the total number of test records, and Boyce indices were averaged arithmetically across the four folds.

The six-predictor Pearson correlation matrix and individual VIF values before BIO04 removal are provided in the S2_6var_Correlation and S2_6var_VIF worksheets of Supplementary Data 1.

S1.2 Tenfold ensembles and all-record models

The main mapping model used random tenfold cross-validation of RM = 2 with QP features across the 246 records. Six folds contained 221 training and 25 test records, and four contained 222 training and 24 test records. The current surface was the arithmetic mean of the ten logistic prediction surfaces. The main MTSPS threshold was 0.2116, the mean of the ten training thresholds. The 10th-percentile training presence (P10) and equal sensitivity and specificity thresholds were 0.2742 and 0.3052, respectively. Future predictions were first averaged across the ten fold-specific projections for each GCM. The resulting surfaces for the three GCMs under the same SSP and period were then averaged with equal weights, and this mean surface was binarized for area calculations. Other tenfold ensembles used their own mean training thresholds: 0.20836 for RM = 2/LQP, 0.16371 for the climate-only RM = 2/QP model, 0.23084 for the climate-plus-elevation RM = 2/QP model, and 0.23901 for the M500 RM = 1/LQ model. The E1+E2 subset, 20 km thinning and three target-group background analyses likewise used their own mean tenfold MTSPS thresholds. Complete thresholds and current and future results are provided in Supplementary Data 1.

To assess the effects of the four configurations selected in the outer folds, each configuration was fitted as a single model using all 246 records and compared with an all-record RM = 2/QP model using the same records, five predictors and national calibration domain. The all-record MTSPS thresholds for QP, LT, P, LQ and QPT were 0.2158, 0.2609, 0.1912, 0.2064 and 0.2723, respectively. Each model was projected to the three GCMs under SSP5-8.5 for 2071–2100. Its continuous surfaces were averaged

and then binarized using its own threshold. In Table S3, Jaccard similarity and differences in current suitable area are relative to the all-record QP model; future increases are relative to each configuration's own current suitable area.

The P-only configuration was evaluated using the all-record RM = 0.5/P model and projections for all three GCMs (Table S3). Its optional tenfold jackknife run ended at the elevation-only submodel because product features require more than one predictor; no complete P-only tenfold ensemble was obtained. Branch-specific results and diagnostic details are provided in S7_P_Diagnostic (Online Resource 2).

Supplementary Methods S2. M500 calibration domain and area accounting

M500 was defined as the intersection of the national extent with the union of 500 km buffers around all 246 records, comprising 210,247 grid cells. This domain was defined from all records before spatial evaluation, and the background was not regenerated within individual folds. The 279 configurations were compared again within M500, yielding RM = 1 with LQ features. Both current and future surfaces were means of tenfold predictions from this configuration. The binary threshold of 0.23901 was the mean tenfold MTSPS threshold; individual fold thresholds ranged from 0.2145 to 0.3036.

Spatial evaluation retained RM = 1 with LQ features and the same four-quadrant partition, with three folds used for training and one for testing. The background remained the predefined M500 domain. Weighted AUC was 0.735, and pooled MTSPS omission was 100/246 (40.7%). These results describe held-out performance under the fixed M500 background and configuration and are reported separately from the national nested-tuning evaluation.

Areas were calculated for three spatial supports: (i) the geographic M500 domain; (ii) the M500 model projected to the full national valid-data domain, without environmental-similarity masking; and (iii) the national projection restricted to paired common environmental support for current and future conditions. For the third calculation, MESS was referenced to the M500 background. If any GCM yielded negative MESS for a pixel, that pixel was removed from both the current and future binary maps. Under SSP5-8.5 at the end of the century, the respective increases were 17.9%, 18.0% and 20.8% (Table S4), each calculated relative to the current suitable area within its own spatial support.

Table S1. Predictions under alternative occurrence-record and background treatments

Analysis	Design	Map r	Current Jaccard	Difference in current area	End-century change under SSP5-8.5
E1+E2 record subset	111 records; fixed RM = 2, QP	0.983	0.941	+5.9%	+17.0%
20 km thinning	168 records; fixed RM = 2, QP	0.995	0.937	+5.6%	+12.9%
Full fern background, σ = 6	246 records; fixed RM = 2, QP	0.971	0.870	+8.3%	+15.5%
Full fern background, σ = 12	246 records; fixed RM = 2, QP	0.988	0.939	+1.5%	+17.2%
Full fern background, σ = 24	246 records; fixed RM = 2, QP	0.972	0.963	−1.8%	+19.4%

Note: Map r, Jaccard similarity and differences in current area are relative to the main tenfold ensemble. End-century changes are relative to each analysis's own current suitable area. Future continuous surfaces averaged across three GCMs were binarized using the corresponding thresholds. The unit of σ is pixels.

Table S2. Mean predictor importance across ten folds

Predictor	Contribution (%)	Permutation importance (%)
BIO11	55.85	46.68
BIO15	19.45	4.90
BIO17	19.04	20.20
Elevation	3.50	25.52
Slope	2.16	2.70

Table S3. Structural comparison of all-record models and end-century predictions under SSP5-8.5

RM/FC	MTSPS threshold	Current area (10^4 km²)	Current Jaccard	Difference in current area (%)	Future increase (%)
2/QP (reference)	0.2158	185.60	1.000	0.0	+15.9
1.5/LT	0.2609	141.63	0.733	−23.7	+12.3
0.5/P	0.1912	184.05	0.746	−0.8	+7.1
0.1/LQ	0.2064	167.82	0.876	−9.6	+21.6
2/QPT	0.2723	144.03	0.745	−22.4	+12.5

Note: Every configuration was a single all-record model using 246 records, five predictors and the national calibration domain. Future increases were calculated after averaging and binarizing continuous surfaces from three GCMs. Differences in current area and Jaccard similarity were calculated relative to the all-record QP model. The all-record QP model serves only as the like-for-like reference in this table; the main-text maps use the tenfold QP ensemble.

Table S4. Changes in suitable area predicted by the M500 model under different spatial supports

Spatial support	Current area (km²)	End-century area (km²)	Increase (%)
Within the geographic M500 domain	1,719,943	2,027,805	+17.9
National valid-data domain, without MESS masking	1,719,943	2,029,497	+18.0
National projection, paired common environmental support relative to M500	1,671,630	2,019,893	+20.8

Note: Future predictions refer to SSP5-8.5 in 2071–2100 and use the M500 tenfold ensemble with a threshold of 0.23901. Paired common-support calculations remove pixels lacking M500 environmental support from both the current and future maps, so their current baseline area differs from that of the unmasked calculation. Areas are rounded for display; percentage increases were calculated from unrounded areas.

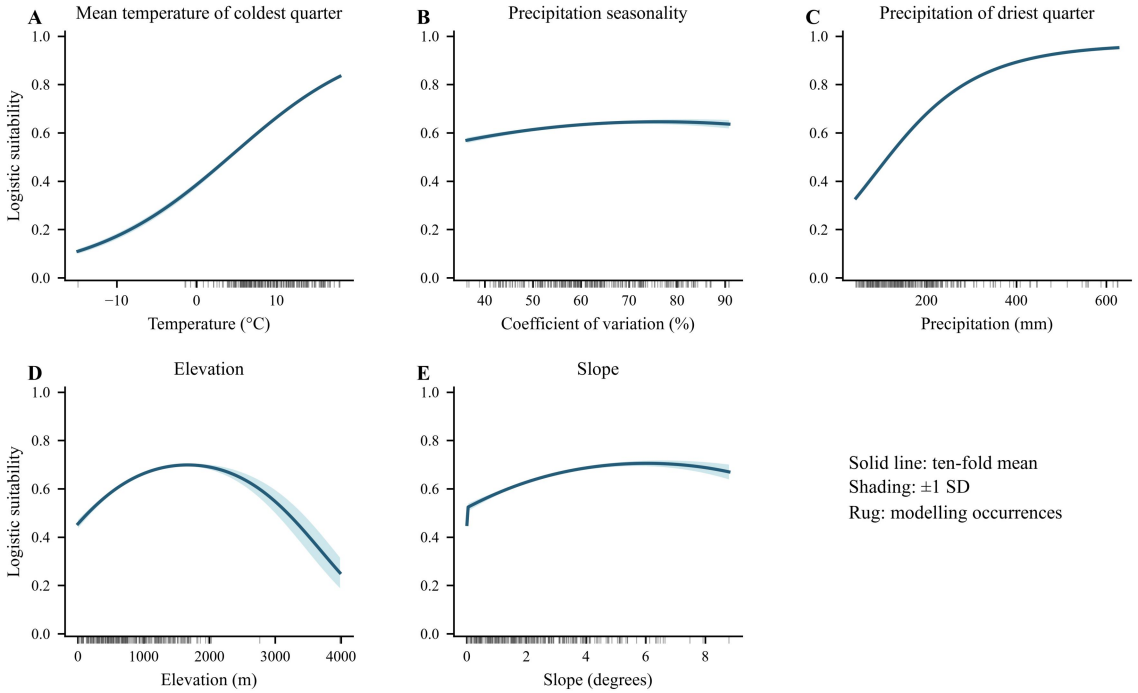

Figure S1. Tenfold marginal response curves for the five predictors. Solid lines show pointwise means of marginal responses across the ten fold-specific models; shading indicates ±1 standard deviation among folds. Rug marks indicate the modelling records.

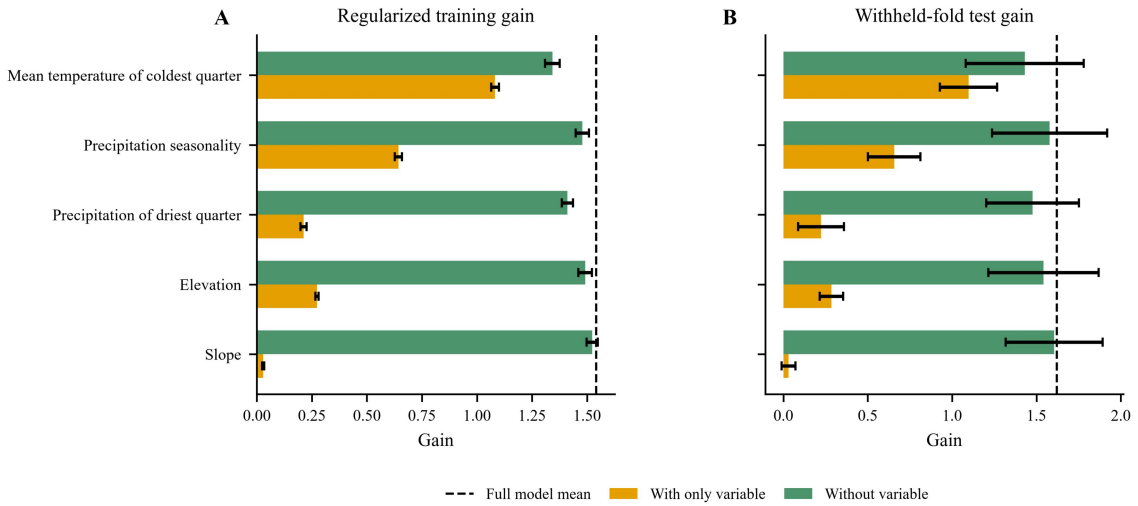

Figure S2. Tenfold Jackknife analysis of the five predictors. Panel A shows regularized training gain, and panel B shows held-out fold test gain. Yellow bars indicate models using only the focal predictor, green bars indicate models excluding it, and the black dashed line shows the mean gain of the full model across ten folds.

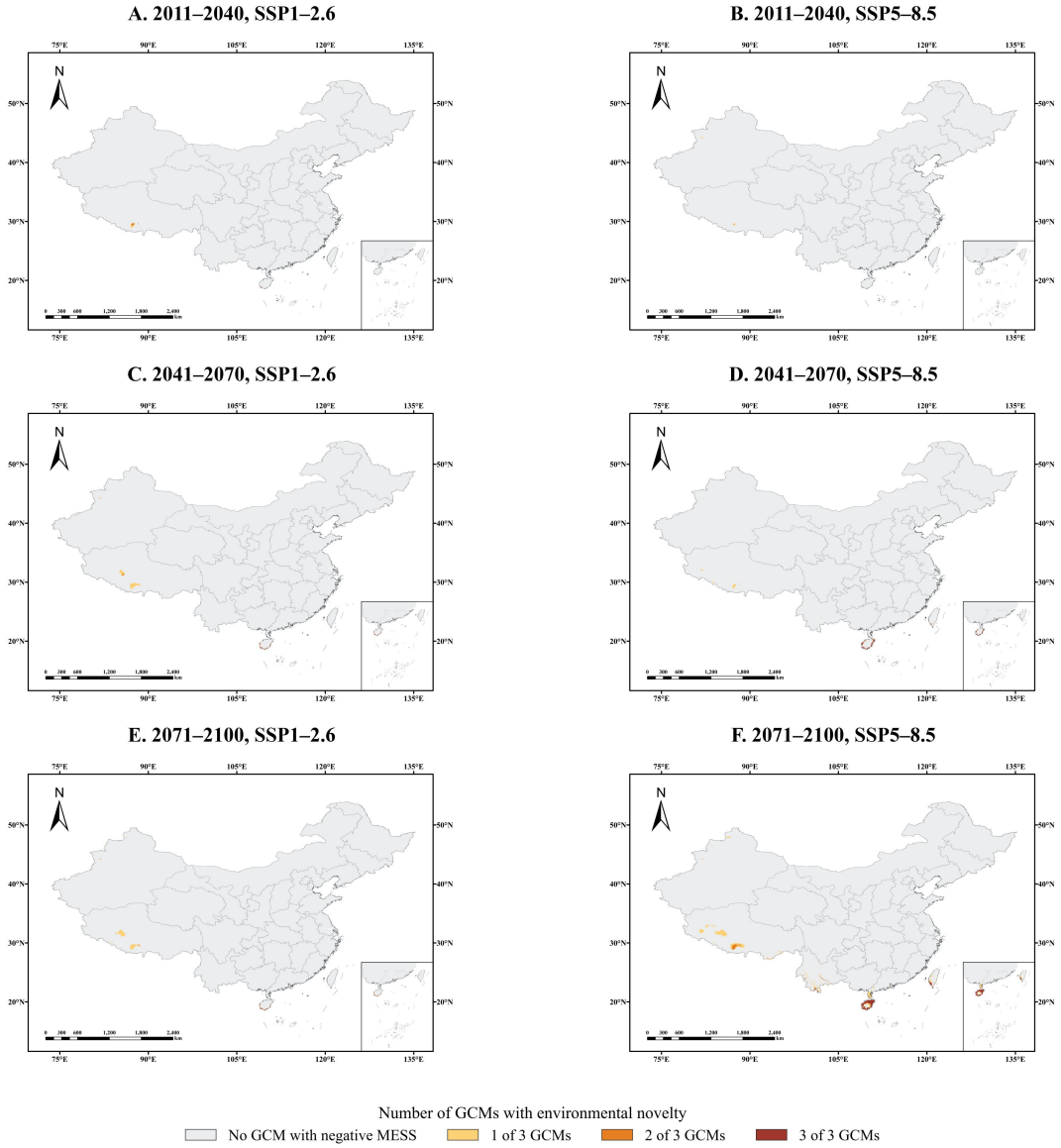

Figure S3. Number of GCMs yielding negative MESS for each future combination.

MESS is referenced to the current national background.

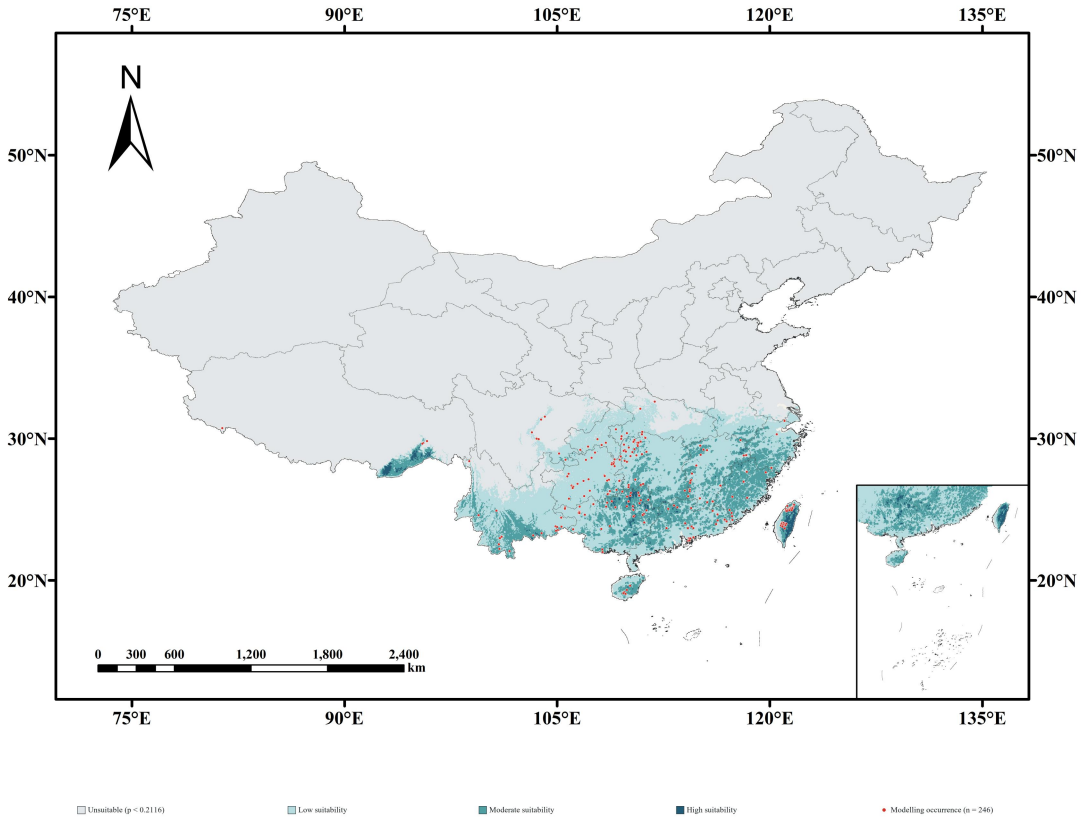

Figure S4. Current macroenvironmental suitability and the 246 modelling records. Light grey indicates unsuitable areas; light blue, turquoise and dark blue indicate low, moderate and high suitability, respectively. Red points show the modelling records. Class thresholds are the same as in main-text Figure 4.

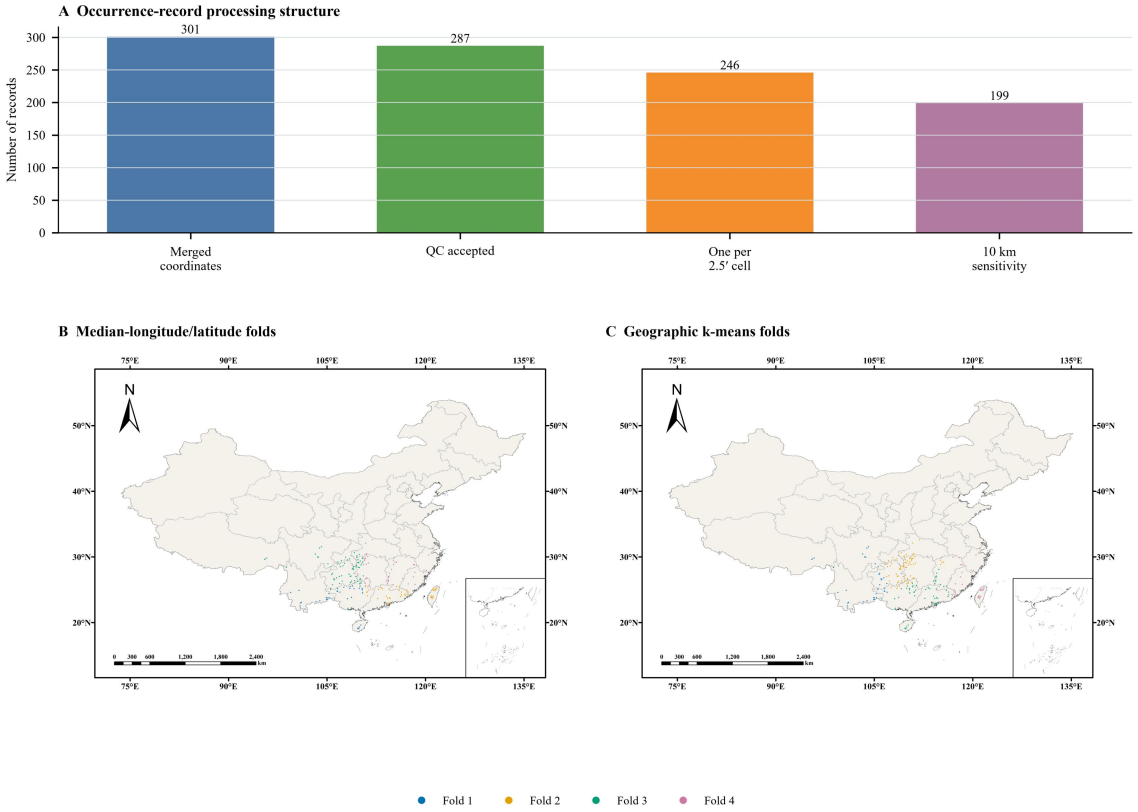

Figure S5. Occurrence-record processing and spatial partitions. Panel A shows changes in record counts, including the supplementary 10-km thinning result (n = 199). Panel B shows the four-quadrant spatial folds used in the main analysis; panel C shows the supplementary geographical k-means partition.

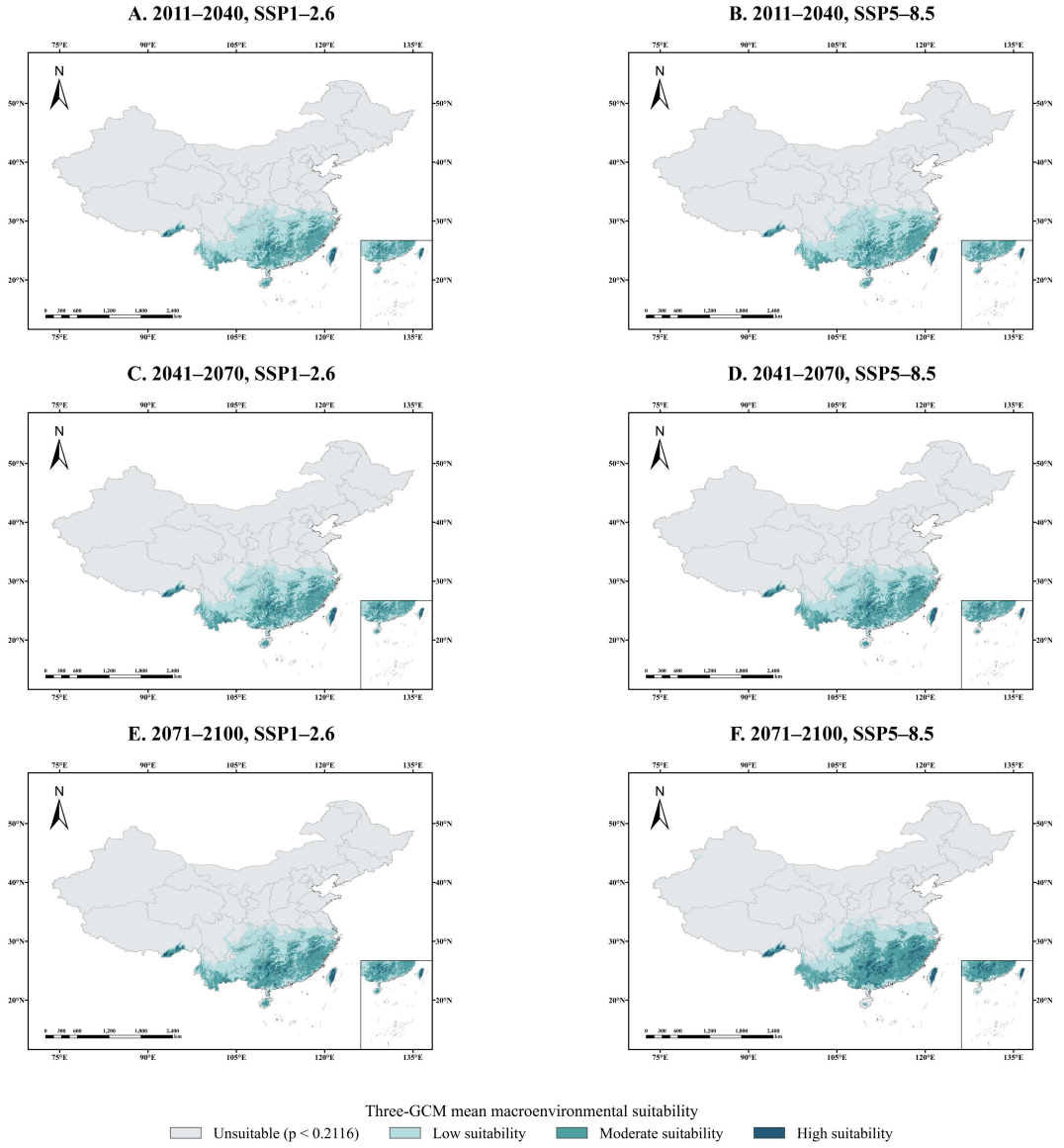

Figure S6. Future absolute suitability under two SSPs and three periods, shown as equally weighted means of continuous prediction surfaces from three GCMs.

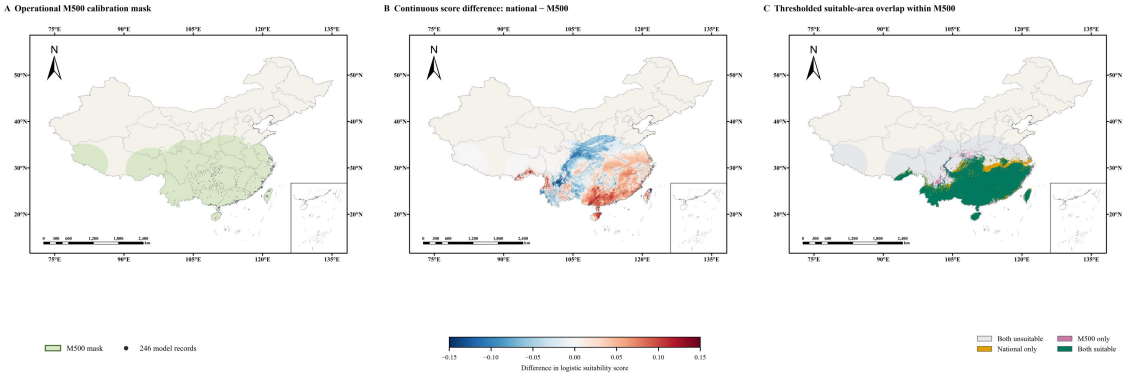

Figure S7. The M500 domain and its current comparison with the national model. In panel A, light green indicates the M500 calibration domain. Panel B shows continuous suitability from the national model minus that from the M500 model: red denotes positive differences and blue negative differences. Panel C shows overlap between binary suitable areas within M500: green indicates suitability under both models, yellow under the national model only, pink under the M500 model only, and light grey under neither model.

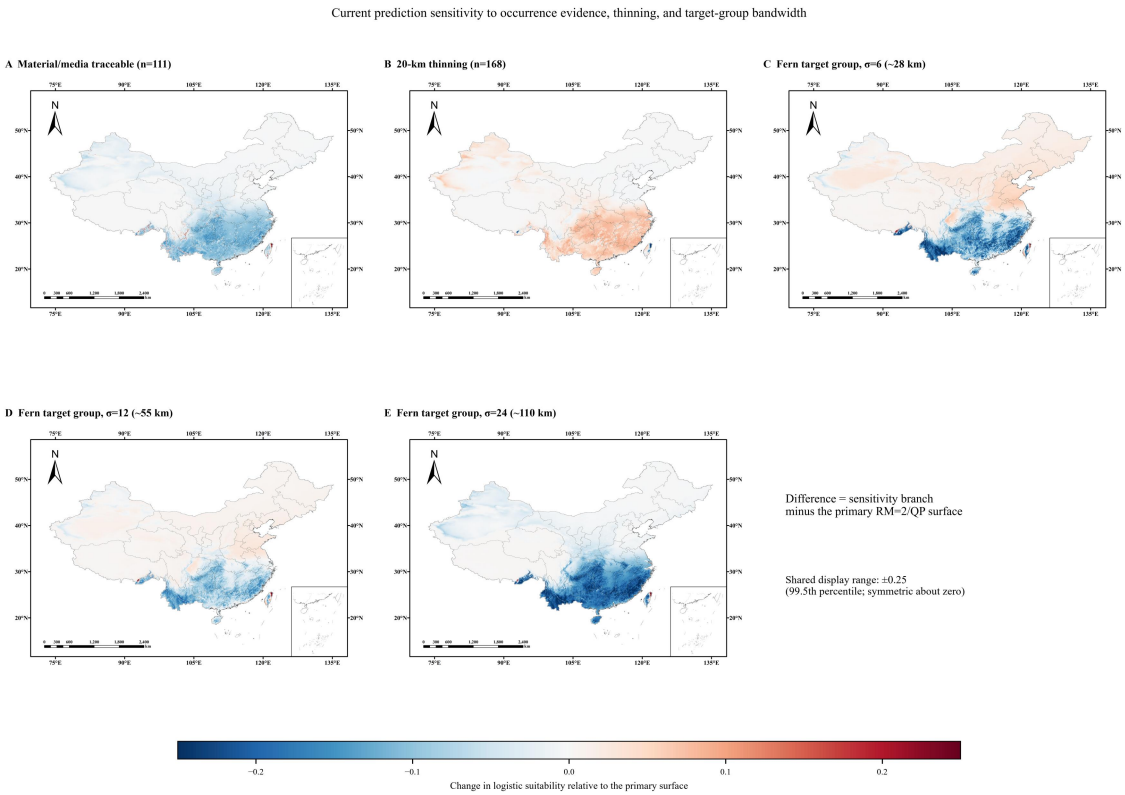

Figure S8. Differences in current logistic suitability from the main RM = 2/QP model with 246 records for analyses using the 111-record E1+E2 subset, 20 km thinning or three bandwidths for the full fern target-group background. All panels use a shared symmetric colour scale centred on 0. Blue indicates lower suitability than in the main model, and red indicates higher suitability.

Supplementary Methods S3. Software and data provenance

S3.1 Software implementations

The analysis environment was recorded on 31 August 2026. The versions below refer to the scientific analyses, not subsequent document preparation. The kuenm 1.1.10 functions were loaded directly from archived R source using sys.source; the project-specific bounded calibration/evaluation code is included with that source in Online Resource 3.

Operation	Implementation and version
Model fitting	MaxEnt 3.4.4; Java 1.8.0_391
Parameter calibration and partial ROC	R 4.6.0; kuenm 1.1.10 source; raster 3.6.32; sp 2.2-1
Scientific scripting	Python 3.14.3
Pearson correlation and VIF	NumPy 2.4.3: corrcoef; inverse correlation matrix
Future raster alignment	Rasterio 1.5.0: reproject; Resampling.bilinear
Environmental similarity	Custom NumPy 2.4.3 implementation of MESS
Area and centroid summaries	NumPy 2.4.3; PyProj 3.7.2 coordinate transforms and WGS84 Geod
Tabular and statistical summaries	Pandas 3.0.1; SciPy 1.17.1
Plots and vector operations	Matplotlib 3.11.0; GeoPandas 1.1.4; Shapely 2.1.2

Online Resource 3 provides the original software snapshot, package versions, scientific entry points and local script dependencies. Its analysis_steps.csv identifies each stage and its input requirements. MaxEnt and Java binaries are obtained separately; the MaxEnt JAR fingerprint is retained in the software record. kuenm source and its derived R evaluation routines retain GPL-2 licensing.

S3.2 Predictor screening and raster alignment

Correlations and VIFs were computed over the common valid cells of the national environmental grid. For standardized predictor columns, VIFs are the diagonal elements of the inverse correlation matrix. The screening limits were absolute Pearson $r < 0.8$ and $VIF < 4$. The six-variable comparison included BIO04, BIO11, BIO15, BIO17, elevation and slope; the final five-variable set excluded BIO04. The corresponding scripts are audit_eco6_stack_20260828.py and stage_redesign_eco5_20260828.py.

S3.2 Predictor screening and raster alignment (continued)

Current analyses used the existing aligned national rasters. Future continuous CHELSA layers were reprojected to that grid by bilinear resampling; elevation and slope were held constant. The model used the stored raster values consistently in current and future inputs. Conversion to physical units uses scale 0.1 and offset -273.15 for BIO11, and scale 0.1 with no offset for BIO15 and BIO17. The archived slope check reproduces the Horn 3 x 3 calculation with a fixed conversion of 111000 m per degree; the latitude-corrected slope is a separate diagnostic.

S3.3 MESS and spatial summaries

For each predictor, the current valid-cell values were sorted. Values inside the reference range were assigned a percentile-based similarity score: twice the percentile below the median and twice its complement above the median. Values outside the range received a negative score proportional to their distance beyond the observed minimum or maximum, divided by the observed range. The minimum score across predictors defined MESS. National and M500 reference distributions were computed separately. The conservative future-only reclassification and paired common-support comparisons follow Methods S1 and S2.

Grid-cell areas were calculated on the WGS84 ellipsoid and summed over thresholded suitable cells. Cell-centre coordinates were transformed to ESRI:102012 for area-weighted centroids, then transformed back to geographical coordinates; centroid-to-centroid distances were calculated with WGS84 geodesics. The scripts analyze_future_transfer_dynamics_redesign_20260828.py and project_future_from_final_lambdas.py contain these calculations.

S3.4 Source files and result reconstruction

Online Resource 2 contains the all-years GBIF source extract, original query URLs and retrieval time, source-dataset attribution and the record-level licence fields. The merged coordinate table and evidence-row index connect source rows to the modelling dataset. The 39-worksheet results workbook is accompanied by product-level environmental metadata, current input fingerprints and a 54-file future-climate source manifest. The manifest distinguishes retained source hashes from the aligned input hashes and identifies URLs reconstructed from the archived acquisition code.

The environmental-source table distinguishes candidate-only soil, vegetation and UV-B products from the five retained predictors. The original access dates remain in the predictor ledger. Product metadata and current source links were checked on 28 October 2026. Provider rasters retain their original terms; source-layer acquisition is documented separately from the author-generated predictions.

Online Resource 3 includes the current tenfold mean and 24 future mean surfaces, together with model coefficients and spatial-fold diagnostics. Its verify_results.py script recalculates current and future suitable areas and pooled nested-spatial evaluation directly from these supplied files, without model refitting. The archived full-analysis scripts and prepare_workspace.py support reuse in a separate workspace after the provider inputs and required software have been supplied.